

(111) oriented (GaAs) n (AlAs) n superlattices are direct band-gap materials for all n's
Su-Huai Wei and Alex Zunger

Citation: *Applied Physics Letters* **53**, 2077 (1988); doi: 10.1063/1.100415

View online: <http://dx.doi.org/10.1063/1.100415>

View Table of Contents: <http://scitation.aip.org/content/aip/journal/apl/53/21?ver=pdfcov>

Published by the *AIP Publishing*

Articles you may be interested in

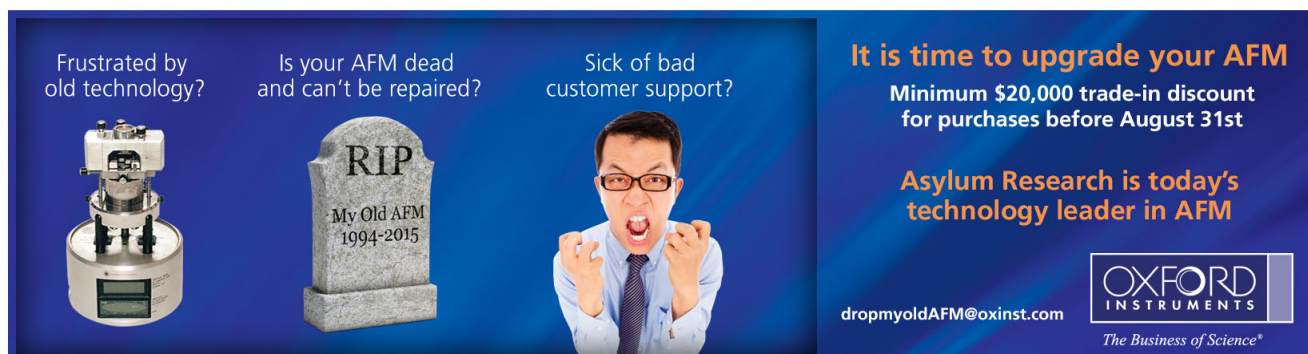
[Super band-gap time-resolved luminescence study of degenerate electron-hole plasma in thin GaAs epilayers](#)
J. Appl. Phys. **80**, 5129 (1996); 10.1063/1.363494

[Polarization dependence of the electroabsorption in low-temperature grown GaAs for above band-gap energies](#)
Appl. Phys. Lett. **68**, 2968 (1996); 10.1063/1.116371

[Screening effects on the band-gap renormalization of strained InGaAs/InGaAsP quantum well lasers lattice matched to GaAs](#)
Appl. Phys. Lett. **68**, 1844 (1996); 10.1063/1.116032

[Energy levels of very short-period \(GaAs\) n -\(AlAs\) n superlattices](#)
Appl. Phys. Lett. **57**, 55 (1990); 10.1063/1.103576

[Nature of the band gap \(direct versus indirect\) of short-period \(GaAs\) n /\(AlAs\) n superlattices grown along the \[111\] confinement direction](#)
Appl. Phys. Lett. **56**, 1233 (1990); 10.1063/1.103333



Frustrated by old technology? Is your AFM dead and can't be repaired? Sick of bad customer support?

It is time to upgrade your AFM
Minimum \$20,000 trade-in discount for purchases before August 31st

Asylum Research is today's technology leader in AFM

dropmyoldAFM@oxinst.com

OXFORD INSTRUMENTS
The Business of Science®

The advertisement features three panels: an old AFM, a tombstone for 'My Old AFM 1994-2015', and a man shouting in frustration. The background is dark blue with light blue accents.

(111) oriented $(\text{GaAs})_n(\text{AlAs})_n$ superlattices are direct band-gap materials for all n 's

Su-Huai Wei and Alex Zunger
Solar Energy Research Institute, Golden, Colorado 80401

(Received 1 August 1988; accepted for publication 20 September 1988)

Total energy calculations show that the (111) $(\text{AlAs})_n(\text{GaAs})_n$ superlattice has a lower formation enthalpy (i.e., is stabler) than either the (001) or (110) superlattices. Self-consistent band structure calculations further show that while the (001) superlattice is direct only for $n > 7$, the (111) superlattice has (i) a smaller and (ii) a *direct* (not pseudodirect) gap for all n 's. Contrary to the expectations based on particle in a box models, the confined states at the zone center are strongly localized even for the monolayer superlattice.

Advances in solid-state lasers, light-emitting diodes, and high-efficiency solar cells have motivated an ongoing search for epitaxial alloys and superlattices with technologically useful *direct* band gaps. The limited success encountered in early¹ molecular beam epitaxy (MBE) growth of (111) films of III-V semiconductors, contrasted with the rapid progress made in achieving low defect densities and good surface morphologies in (100) films,² established the tradition of using (100) structures, almost to the exclusion of any other orientation, in a wide range of devices. Inspired by this early elimination process, most theoretical investigations of III-V superlattices have focused on this particular orientation (Ref. 3, and references therein). More recently, the advent of zinc-blende on diamond-type heterostructures (e.g., GaAs/Ge, GaP/Si) renewed interest in nontraditional growth directions for III-V's, including the (211),⁴ (311),⁵ and (110).⁶ Substantial progress has recently been made also in (111) growth of GaAs-AlAs quantum well structures,^{7,8} exhibiting a higher radiative efficiency than the traditional (100) oriented structure.⁸ This progress, as well as new observations of *spontaneous* ordering of III-V alloys into short-period (111) oriented superlattice-like phases,⁹ is now motivating theoretical calculations of stability and band gaps of lattice-mismatched¹⁰ and lattice-matched (111) superlattices. While the $\text{Al}_{0.5}\text{Ga}_{0.5}\text{As}$ alloy has an indirect band gap near¹¹ X , and the (001) oriented $(\text{AlAs})_n(\text{GaAs})_n$ superlattice³ is indirect at an L -folded state for $n = 1$ and indirect at an X -folded state for $1 < n \leq 7$, we find that the (111) oriented $(\text{AlAs})_n(\text{GaAs})_n$ superlattice has a direct band gap for all n values, from ~ 1.97 eV at $n = 1$, converging to the GaAs bulk value of 1.52 eV for large n 's. We describe here the first *ab initio* calculation of the electronic structure of (111) oriented $(\text{AlAs})_n(\text{GaAs})_n$ superlattices, and identify a novel physical mechanism which clarifies why this superlattice is direct although short-period $(\text{AlAs})_n(\text{GaAs})_n$ (001) superlattices are indirect.

We have used the first-principles self-consistent all-electron local density formalism, as implemented by the linear augmented plane wave (LAPW) method¹² to calculate the total energies and band structures for short-period (001) and (111) oriented $(\text{AlAs})_n(\text{GaAs})_n$ superlattices. Defining the formation enthalpy of an n -period $(AC)_n(BC)_n$ superlattice in the orientation G as its total energy relative to

equivalent amounts of its binary constituents (per four atoms)⁴

$$\Delta H(n,G) = (1/n)E[(AC)_n(BC)_n;G] - E[AC] - E[BC], \quad (1)$$

we find: (i) for $n = 1$, $\Delta H(001) = \Delta H(110) = 11.4$ meV/(four atoms), but $\Delta H(111) = 7.5$ meV/(four atoms), so that the (111) alternate monolayer superlattice is thermodynamically stabler than the other two $n = 1$ superlattices. (ii) As the superlattice period n increases, $\Delta H(n,G)$ decreases for all orientations, so the stability is enhanced. However, the rate of this decrease depends on the orientation G . Assuming that the interaction energies beyond the fourth cation-cation neighbor are negligible, we find that past a critical repeat period n_c [2 for (001) and (111) oriented superlattices but 4 for the (110) oriented system]

$$\Delta H(n,G) = 2I(G)/n, \quad n \geq n_c, \quad (2)$$

where $I(G)$ is the "interface energy." Our total energy calculations yield (in meV)

$$I[001] = 3.6, \quad I[110] = 5.8, \quad I[111] = 2.7, \quad (3)$$

showing that the (111) oriented superlattice is not only stabler than the other two orientations for $n = 1$, but indeed it is stabler for all n values. Note that (110) superlattices are predicted to be thermodynamically the most unstable towards disproportionation into binary constituents in this group.⁶

Our strategy for obtaining trends in the energy levels of different superlattices is as follows. First, we calculate the bulk energy levels of GaAs and AlAs on a common energy scale using the valence-band offset $\Delta E_v = 0.45$ eV we obtained earlier¹³ with the same LAPW method. This establishes the energies of the various conduction-band potential wells, hence also the band edges to which superlattice energy levels will converge in the limit of very large ($n \rightarrow \infty$) repeat periods. Second, we calculate self-consistently the electronic structure of $n = 1$ and 2 superlattices in the (001) and (111) orientations, placing these levels on the same common energy scale deduced from the binary bulk systems. This establishes the electronic structure, wave-function localization, and direct/indirect nature of the transitions. Finally, given the results for $n = 1, 2$ and $n = \infty$, we identify qualitative trends of energy levels ϵ with n , assuming that for intermedi-

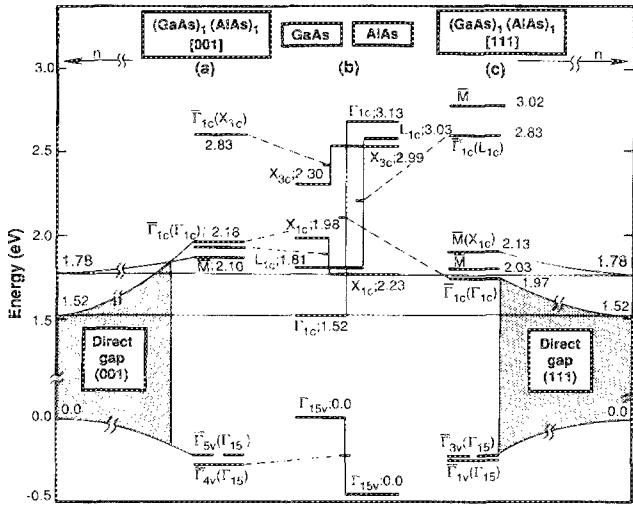


FIG. 1. Calculated energy levels (in eV) of $(\text{AlAs})_1(\text{GaAs})_n$ at high symmetry points for the (a) (001) and (c) (111) orientations. (b) shows the energy levels of bulk GaAs and AlAs on a common energy scale. The dashed line connecting the centers of the various potential wells in (b) to the superlattice energy levels in (a) and (c) denote the level repulsion effect. The far right and far left parts of the figure show schematically the convergence, as a function of repeat period n , of the superlattice energy levels to the bulk band edges. The (111) superlattices are direct for all n , whereas the (100) superlattices are direct only past $n > 7$.

at n values $\epsilon \sim 1/n^2$ (our main conclusions, however, do not draw heavily on the details of this scaling).

Figures 1(a) and 1(c) depict the calculated energy levels at some high symmetry points in the Brillouin zone for the $n = 1$ (001) and (111) superlattices, respectively. These energy levels were corrected for the local density band-gap error according to the procedure described earlier.³ We have denoted in Fig. 1 the superlattice labels with an overbar, indicating in parentheses the zinc-blende states from which they fold. We see that in the (001) superlattice the X -folded states $\bar{M}(X_{x,y})$ and $\bar{\Gamma}_4(X_z)$ are at $E_v + 2.10$ eV and $E_v + 2.17$ eV, respectively, both lower in energy than the direct superlattice state $\bar{\Gamma}_{1c}(\Gamma_{1c})$ at $E_v + 2.18$ eV. The conduction-band minimum [not shown in Fig. 1(a)] in this case is at $\bar{R}_{1c}(L_{1c})$ (i.e., the superlattice state folded from L_{1c}) at $E_v + 1.93$ eV. In contrast, in the (111) oriented superlattice the conduction-band minimum (CBM) is the direct $\bar{\Gamma}_{1c}(\Gamma_{1c})$ state at $E_v + 1.97$ eV, while the X - and L -folded states (denoted as \bar{M}) are higher in energy at $E_v + 2.03$ eV and 2.13 eV, respectively. It is easy to see that the (111) superlattice will remain direct for $n > 1$, while the (001) superlattice will exhibit a direct/indirect crossover. As the superlattice period increases, all states eventually approach the corresponding potential well minima of the binary constituents. Specifically, the $\bar{\Gamma}(\Gamma_{1c})$ superlattice level in both orientations approaches the value of the direct gap of GaAs (1.52 eV at low temperature), whereas the X_{1c} -derived $\bar{\Gamma}(X_{1c})$ and $\bar{M}(X_{1c})$ states in the (001) oriented superlattices approach the bulk AlAs X_{1c} energy [2.23 eV above the AlAs valence-band maximum (VBM), or $2.23 - \Delta E_v = 1.78$ eV above the GaAs VBM]. We indicate these trends schematically on the right- and left-hand sides of Fig. 1 [see Ref. 3 for more detailed results for $n > 1$ in (001) superlattices]. In the $n = 1$ (111) superlattice, the $\bar{\Gamma}_{1c}(\Gamma_{1c})$ state at

$E_v + 1.97$ eV is lower in energy than the \bar{M} superlattice state at $E_v + 2.03$ eV. For $n = 2$ the values are $E_v + 2.08$ eV and $E_v + 2.15$ eV, respectively. Since as n increases, $\bar{\Gamma}_{1c}(\Gamma_{1c})$ approaches $E_v + 1.52$ eV, while \bar{M}_c approaches a higher value of $E_v + 1.78$ eV, this superlattice will remain direct for all n .¹⁴ In contrast, in the $n = 1$ (001) superlattice, $\bar{\Gamma}_{1c}(\Gamma_{1c})$ at $E_v + 2.18$ eV is higher in energy than the \bar{M} state at $E_v + 2.10$ eV. Since as n increases, $\bar{\Gamma}_{1c}(\Gamma_{1c})$ approaches $E_v + 1.52$ eV whereas \bar{M}_c approaches the higher value of $E_v + 1.78$ eV, this system will remain indirect until $\bar{\Gamma}_{1c}$ and \bar{M}_c cross after which it will become direct.

Three unexpected (and related) effects are evident in our results: (i) the (111) oriented superlattice is direct (not pseudodirect), while the (001) oriented superlattice is indirect for small n values; (ii) the (111) superlattice has a considerably smaller $\bar{\Gamma}_v \rightarrow \bar{\Gamma}_c$ gap than the (100) superlattice (Fig. 1); and (iii) despite a very light electron effective mass m^* at $\bar{\Gamma}_{1c}$ ($\sim 0.07m$), which in simple square-well or Kronig-Penney models would suggest for the $n = 1$ superlattice an enormous upward shift of the confined level and extensive wave-function delocalization, we find the $\bar{\Gamma}_{1c}(\Gamma_{1c})$ states in either orientation to be only 0.45–0.66 eV above the bulk GaAs CBM and to exhibit substantial wave-function localization on the Ga-As sublattice (Fig. 2).

We find a simple explanation to these phenomena in terms of a "quantum level repulsion effect," ignored by other simple models. Symmetry considerations show that the zinc-blende X_{3c} state in the $n = 1$ common-anion (001) oriented superlattices folds into $\bar{\Gamma}_{1c}(X_{3c})$, whereas the zinc-blende Γ_{1c} state folds into itself, creating $\bar{\Gamma}_{1c}(\Gamma_{1c})$. Since both folded states have the same (Γ_1) symmetry representation, in perturbation theory they repel each other by an amount

$$\delta E = \pm \frac{|\langle m, k | \Delta V | m', k' \rangle|^2}{\epsilon_m(k) - \epsilon'_m(k')} \quad (4)$$

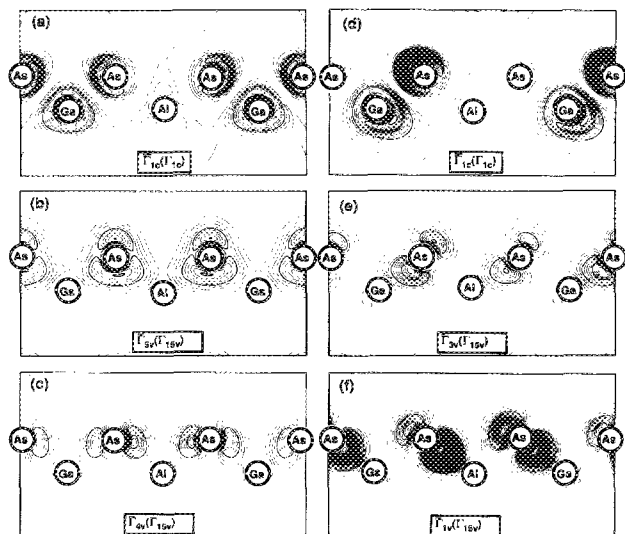


FIG. 2. Calculated electronic charge density contours for the conduction-band $\bar{\Gamma}_{1c}(\Gamma_{1c})$ and the doubly degenerate $(\Gamma_{5v}, \Gamma_{3v})$ valence-band and single (Γ_{1v}) states in $(\text{AlAs})_1(\text{GaAs})_n$ superlattices. Note the higher localization on the Ga site in (d) (111) relative to (a) (001) superlattices, and the existence of significant anion character in these states. The valence states have mostly p -like character on As. The contour increment is $4 \times 10^{-3} e/a.u.^3$.

where $|m, \mathbf{k}\rangle$ and $|m', \mathbf{k}'\rangle$ are the zinc-blende states (for band m and wave vector \mathbf{k}) folding in the superlattice into the same representation, and $\Delta V(\mathbf{r})$ is the ordering potential. Since the energy denominator for the $\bar{\Gamma}_{1c}$ -folded states in GaAs-AlAs is relatively large (the difference between the average X_{3c} and the average Γ_{1c} energies of GaAs and AlAs at low temperatures is $2.645 - 2.325 = 0.32$ eV), this level repulsion is relatively weak in the (001) superlattice [± 0.15 eV in Fig. 1(a)]. In fact, this downward repulsion of $\bar{\Gamma}_{1c}(\Gamma_{1c})$ is insufficient to push this state below the indirect $\bar{M}(X_{1c})$ edge (which experiences negligible repulsion and remains near the X_{1c} well center energy of 2.10 eV). The situation is qualitatively different in the $n = 1$ (111) oriented superlattices, where symmetry mandates folding of L (not X) into $\bar{\Gamma}$, yielding in the superlattice the isosymmetry pair $\bar{\Gamma}_{1c}(L_{1c})$ and $\bar{\Gamma}_{1c}(\Gamma_{1c})$ which again repel each other. Here, however, the energy denominator of Eq. (4) is more than three times smaller than the (001) value (the difference between the average L_{1c} and the average Γ_{1c} energies of GaAs and AlAs is only $2.42 - 2.325 = 0.095$ eV). Indeed, this $\bar{\Gamma}_{1c} - L_{1c}$ level repulsion is so strong in the (111) superlattice that it pushes $\bar{\Gamma}_{1c}(\Gamma_{1c})$ downward even below the indirect $\bar{M}(L_{1c} + X_{3c})$ state at 2.03 eV, making the system direct. In general, a downward repulsion of a level [here, $\bar{\Gamma}_{1c}(\Gamma_{1c})$] is associated with enhanced localization on the sublattice with the lower energy quantum well (here, GaAs). Figure 2 compares the calculated charge densities of the $\bar{\Gamma}_{1c}(\Gamma_{1c})$ state in the (001) and (111) monolayer superlattices, showing clearly greater localization in (111) relative to the (001) superlattice, owing to the greater level repulsion in the former case.

In general, we expect a switching between indirect gap in (001) to direct gap in (111) for systems whose 50%-50% average energies have the sequence $X_{1c} < \Gamma_{1c} < L_{1c} < X_{3c}$, with small $\Gamma_{1c} - L_{1c}$ and large $\Gamma_{1c} - X_{3c}$ energy splittings [see Eq. (4)]. In such cases, the larger $L_{1c} - \Gamma_{1c}$ level repulsion attendant upon (111) ordering may push Γ_{1c} below X_{1c} and become the CBM, whereas the weaker $X_{3c} - \Gamma_{1c}$ level repulsion characteristic of (001) common-anion ordering is insufficient to make Γ_{1c} the CBM [for common-cation (001) ordering, repulsion between $X_{1c} - \Gamma_{1c}$ can make the system only *pseudodirect*]. AlAs-GaAs and GaP-GaAs appear to satisfy these conditions.

Since the early days of semiconductor superlattices, it has been customary¹⁵ to rationalize trends in superlattice energy levels in terms of confinement of wave functions into

wells of finite dimension d , leading to an increase in the kinetic energy, hence to an upward shift of the energy levels in proportion to $(m^*d^2)^{-1}$. Simple particle in a box, Kronig-Penny, effective mass, and envelope function models commit to this basic notion of the overriding importance of *kinetic energy* effects. Our calculation, treating superlattices as ordinary crystals in their own right in a band-theoretic approach (using potential and kinetic energies on an equal footing), illustrates the basic shortcomings of these approaches for ultrathin superlattices: even though on the basis of kinetic energy considerations (the values of m^* and d) one would have judged the superlattice states $\bar{\Gamma}_{1c}(\Gamma_{1c})$ to be displaced substantially *upward* from the well bottom, and, hence, to become *delocalized*, quantum repulsion effects [reflecting the role of potential energy, see Eq. (4)] counteract the kinetic confinement effect, leading to a *lowering* of the energy level towards the band edge and to significant wavefunction *localization*.

- ¹A. Y. Cho, J. Appl. Phys. **41**, 2780 (1970).
- ²See, H. C. Casey and M. B. Panish, *Heterostructure Lasers* (Academic, New York, 1978).
- ³S.-H. Wei and A. Zunger, J. Appl. Phys. **63**, 5794 (1988) gives an extensive list of recent calculations on (001) oriented (AlAs)_n(GaAs)_n superlattices and compared them with recent experimental data.
- ⁴S. Subbanna, H. Kroemer, and J. L. Merz, J. Appl. Phys. **59**, 488 (1986); W. I. Wang, Surf. Sci. **174**, 31 (1986).
- ⁵W. I. Wang, T. S. Kuen, E. E. Mendez, and L. Esaki, Phys. Rev. B **31**, 6890 (1985).
- ⁶W. I. Wang, J. Vac. Sci. Technol. B **1**, 630 (1983).
- ⁷T. Fukunaga, T. Takamori, and H. Nakashima, J. Cryst. Growth **81**, 85 (1987).
- ⁸T. Hayakawa, K. Takahashi, M. Kondo, T. Suyama, S. Yamamoto, and T. Hijikata, Phys. Rev. Lett. **60**, 349 (1988).
- ⁹Y. E. Ihm, N. Otsuka, J. Klem, and H. Morkoç, Appl. Phys. Lett. **51**, 2013 (1987); A. Gomyo, T. Suzuki, and S. Iijima, Phys. Rev. Lett. **60**, 2645 (1988); M. Kondow, H. Kakibayashi, and S. Minagawa, J. Cryst. Growth **88**, 291 (1988); M. A. Shahid, S. Mahajan, D. E. Laughlin, and H. M. Cox, Phys. Rev. Lett. **58**, 2567 (1987).
- ¹⁰C. Mailhot and D. L. Smith, Phys. Rev. B **35**, 1242 (1987).
- ¹¹M. D. Sturge, E. Cohen, and R. A. Logan, Phys. Rev. B **27**, 2362 (1983).
- ¹²S.-H. Wei and H. Krakauer, Phys. Rev. Lett. **55**, 1200 (1985), and references therein.
- ¹³S.-H. Wei and A. Zunger, Phys. Rev. Lett. **59**, 144 (1987). This value has but a weak orientation dependence (see Ref. 5). The small uncertainty in ΔE_v (~ 0.1 eV) will not change our conclusion.
- ¹⁴Dr. E. Yamaguchi has informed us in a private communication, for which we are grateful, that his preliminary tight-binding calculations also show the (111) oriented (AlAs)_n(GaAs)_n superlattice to be direct for $3 < n < 18$.
- ¹⁵L. Esaki and R. Tsu, IBM J. Res. Devel. **14**, 61 (1970).